*Electrochemical and Solid-State Letters*, **9** (12) G354-G357 (2006)
1099-0062/2006/9(12)/G354/4/$20.00 © The Electrochemical Society

# Interstitial-Mediated Arsenic Clustering in Ultrashallow Junction Formation

**Scott A. Harrison, Thomas F. Edgar, and Gyeong S. Hwang**[z]

*Department of Chemical Engineering, University of Texas, Austin, Texas 78713*

We propose a viable route for interstitial-mediated formation of arsenic-vacancy clusters that are primarily responsible for arsenic deactivation in the fabrication of ultrashallow junctions in Si, based on first-principles density functional calculations for the stability of arsenic-defect clusters. We present the atomic structures and binding energies of newly identified neutral arsenic-interstitial complexes ($As_mI_n$, $m \leq 6$ and $n \leq 3$), with comparison to the energetics of arsenic-vacancy complexes ($As_mV_n$, $m \leq 6$ and $n \leq 2$). Based on these results, we discuss the relative role of interstitials and vacancies in arsenic deactivation during ultrashallow junction formation.
 [DOI: 10.1149/1.2359084] 

Manuscript submitted June 1, 2006; revised manuscript received August 3, 2006. Available electronically October 5, 2006.

As metal-oxide semiconductor field effect transistor (MOSFET) scaling continues, sophisticated vertical and lateral channel engineering is required to minimize short channel effects. In addition, precise optimization of dopant profiles is necessary to improve device performance. At present, ultrashallow junction fabrication typically involves low-energy, high-dose dopant implantation followed by a high-temperature thermal anneal. During the postimplantation annealing, implanted dopants may undergo transient enhanced diffusion (TED) and agglomeration, which can lead to severe dopant profile broadening and deactivation. A deeper understanding of mechanisms underlying the dopant diffusion and clustering is therefore necessary to find optimum processing conditions for the successful fabrication of next-generation devices.

In highly As-doped Si regions, the concentration of free electrons tends to saturate at the level of approximately $2 \times 10^{20}$ $cm^{-3}$.[1] Theoretical studies have identified $As_3V$, $As_4V$, $As_2V_2$, and $As_3V_2$ complexes that may play a major role in As deactivation.[2-4] Indeed, the formation of stable As-vacancy clusters has been observed in highly-As-doped regions.[5-7] Based on these observations, a kinetic model of vacancy-mediated As diffusion and agglomeration has been proposed to explain the As TED and electrical deactivation.[8]

However, little is known about the role of interstitials, although they are expected to exist in excess[9] and assist in arsenic-enhanced diffusion[10-12] during postimplantation annealing. Recent theoretical studies have predicted that enhanced diffusion may occur via a mobile As-interstitial pair.[13] The existence of this mobile pair along with the ease of As-vacancy complex annihilation by interstitial-vacancy recombination,[14] leads to the possibility of As-interstitial clustering in interstitial-rich regions. In addition, recent experimental investigations have demonstrated that the density of extended {311} defects in Si decreases with the concentration of As, implying the formation of stable As-interstitial complexes.[15,16]

In this letter, we propose an interstitial-assisted pathway for the formation of electrically inactive As-vacancy complexes during thermal processing of ultrashallow implanted As junctions. We first determine the minimum-energy structure and formation energies of As-interstitial complexes ($As_mI_n$, $m \leq 6$ and $n \leq 3$) and then compare their stability with As-vacancy clusters ($As_mV_n$, $m \leq 6$ and $n \leq 2$). Based on the results, we present a potential energy map for As-defect clusters (*vide infra*). This demonstrates that not only vacancies but also interstitials can be responsible for As deactivation. However, given the fact that interstitials are present in excess during postimplantation annealing, particularly at the early-stage annealing, we expect that the As deactivation would mainly occur through the interstitial-assisted route.

All atomic and electronic structures and total energies were calculated using the plane-wave basis pseudopotential method within the generalized gradient approximation (PW91 GGA)[17] to density functional theory (DFT), as implemented in the Vienna Ab-initio Simulation Package (VASP).[18] We use Vanderbilt-type ultrasoft pseudopotentials[19] and a planewave cutoff energy of 12 Ry. The As-interstitial complexes computed here are modeled using a 64 atom supercell while the As and As-vacancy complexes use a 216 atoms cell. In both cases, a fixed lattice constant of 5.457 Å was used. All atoms were fully relaxed using the conjugate gradient method until residual forces on constituent atoms became smaller than $5 \times 10^{-2}$ eV/Å. A $4 \times 4 \times 4$ mesh of k points in the scheme of Monkhorst–Pack was used for the Brillouin zone sampling.[20]

In Table I, we summarize the computed relative formation energies for As-defect clusters in crystalline Si, which are given by

$$E_f = E[As_mSi_n] - m\mu_{As}n\mu_{Si}$$

where $E[As_mSi_n]$ is the total energy of the supercell containing $m$ As atoms and $n$ Si atoms, $\mu_{As}$ is the relative energy per neutral substitutional As atom in bulk Si, and $\mu_{Si}$ is the energy per bulk Si atom. For a given supercell with $N$ lattice sites ($N = 64$ or 216), the complexes where $m + n = N$ indicates substitutional As aggregates with no defects ($As_m$). When $m + n > N$, the interstitial (I) number is given $m + n - N$, while if $m + n < N$, the number of vacancies ($V$) is given by $N - (m + n)$. For the neutral Si interstitial, we only consider the lowest-energy (110)-split state. Our calculated formation energies of As-vacancy complexes (containing up to four As atoms) and silicon interstitial clusters are in good agreement with previous theoretical results available in literature,[2-4,21,22] as are the energies for AsI[13] and $As_2I$[23]. While the $As_2I$ and $As_4I$ complexes were reported in an early study,[3] the local-minimum structures we present here are likely to give formation energies significantly below those reported previously.

**Table I. Relative formation energies of defect, arsenic, and arsenic-defect complexes with respect to neutral substitutional arsenic.**

| | $E_f$ | | $E_f$ | | $E_f$ |
|---|---|---|---|---|---|
| $V_2$ | 5.37 | V | 3.60 | | |
| $AsV_2$ | 3.99 | AsV | 2.34 | As | 0 |
| $As_2V_2$ | 2.44 | $As_2V$ | 0.75 | $As_2$ | 0.14 |
| $As_3V_2$ | 1.32 | $As_3V$ | −0.36 | $As_3$ | 0.34 |
| $As_4V_2$ | −0.29 | $As_4V$ | −1.93 | $As_4$ | −0.17 |
| $As_5V_2$ | −1.39 | $As_5V$ | −1.80 | $As_5$ | −0.05 |
| $As_6V_2$ | −2.99 | $As_6V$ | −1.61 | $As_6$ | −0.37 |
| I | 3.79 | $I_2$ | 5.69 | $I_3$ | 7.22 |
| AsI | 3.19 | $AsI_2$ | 5.10 | $AsI_3$ | 6.72 |
| $As_2I$ | 2.12 | $As_2I_2$ | 4.51 | $As_2I_3$ | 5.90 |
| $As_3I$ | 2.11 | $As_3I_2$ | 4.17 | $As_3I_3$ | 5.78 |
| $As_4I$ | 1.46 | $As_4I_2$ | 3.16 | $As_4I_3$ | 5.09 |
| $As_5I$ | 1.47 | $As_5I_2$ | 3.17 | $AS_5I_3$ | 5.10 |
| $As_6I$ | 1.38 | $As_6I_2$ | 3.17 | $As_6I_3$ | 4.40 |

[z] E-mail: gshwang@che.utexas.edu

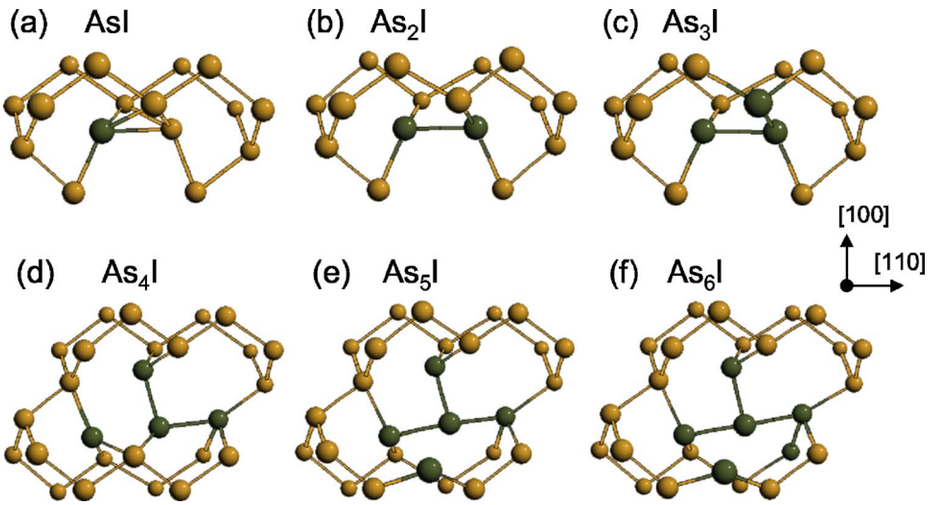


**Figure 1.** (Color online) $As_mI$ complex structures. The arsenic and silicon atoms are given by dark- (green) and light- (yellow) colored atoms, respectively.

Next, we discuss the minimum energy configurations of neutral As-interstitial clusters that were identified from our extensive search. To confirm the minimum-energy state of each structure, we also performed ab initio molecular dynamics based on the Born–Oppenheimer approach for at least 5 ps at 1300 K, followed by static structural optimization.

Figure 1 shows the minimum-energy structures of neutral $As_mI$ clusters ($m \leq 6$). The minimum energy AsI pair [(a)] is comprised of As and $Si_i$ atoms that are aligned in the [110] direction while sharing a lattice site,[13] while the lowest-energy structure of $As_2I$ [(b)] consists of two As atoms bonded together in a single lattice site with a bond axis which is tilted slightly from the [110] direction.[23] The threefold coordinated As atoms in these two structures each carry an electron lone pair. We find the $As_3I$ [(c)] complex has a similar structure to the $As_2I$ complex, with two As atoms being threefold coordinated. The $As_4I$ [(d)] structure contains three, while the $As_5I$ [(e)] and $As_6I$ [(f)] structures contain four threefold coordinated As atoms (with a lone electron pair each).

Figure 2 shows the lowest-energy structures of neutral $As_mI_2$ clusters ($m \leq 6$). Starting with the minimum-energy configuration of $I_2$[21] we carefully examined all possible atomic structures of $AsI_2$ [(a)], $As_2I_2$ [(b)], and $As_3I_2$ [(c)] clusters, which turn out to resemble the interstitial dimer. We then identified the minimum-energy $As_4I_2$ structure in which the As atoms are chained together to occupy two adjacent Si lattice sites [(d)]. This structure is a natural extension of the $As_2I$ complex in the [110] direction, here all As atoms are threefold coordinated. We also examined the stability of $As_5I_2$ [(e)] and $As_6I_2$ [(f)] clusters by placing additional substitutional As atoms in the vicinity of the $As_4I_2$ structure. However, there is no significant energy gain by the agglomeration.

Figure 3 shows the lowest-energy structures of neutral $As_mI_3$ clusters ($m \leq 6$). We first used the extended $I_3$ configuration[21] to determine the minimum-energy $AsI_3$ [(a)], $As_2I_3$ [(b)], and $As_3I_3$ [(c)] structures. Note that for $I_3$ the extended structure is predicted to be slightly energetically more favorable than the compact structure.[21] We also examined $AsI_3$, $As_2I_3$, and $As_3I_3$ structures using the compact $I_3$ structure as a basis but found these structures less energetically favorable than those formed from the extended structure as well. Next, we determined a chained structure for $As_6I_3$ [(f)] in which all As atoms are linked together in threefold coordination (with a lone electron pair each) while occupying three adjacent Si lattice sites. Using this structure as a starting point, we identified minimum-energy configurations for $As_4I_3$[(d)] and $As_5I_3$ [(e)] complexes.

Based on the formation energies of As-defect complexes examined, we present a potential energy map for As agglomeration in Fig.

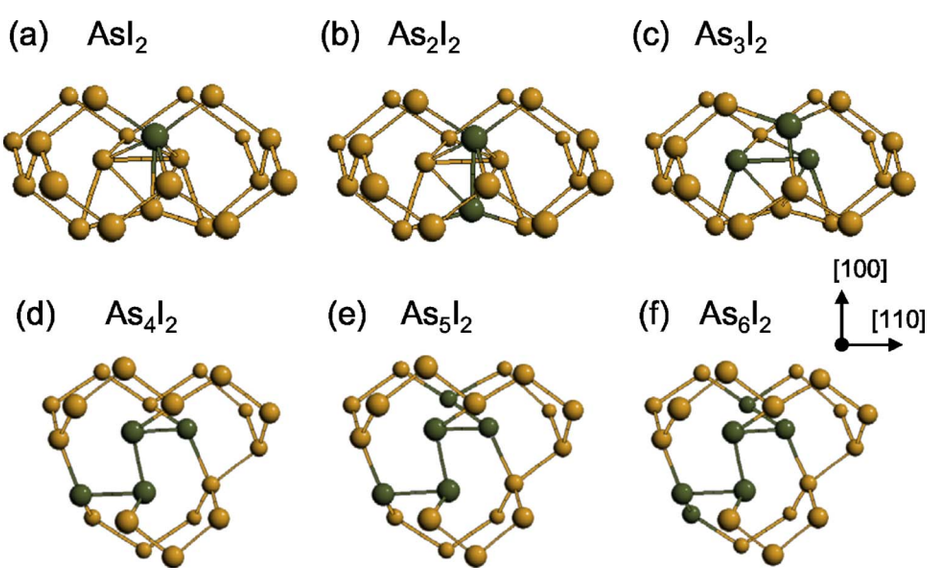


**Figure 2.** (Color online) $As_mI_2$ complex structures. The arsenic and silicon atoms are given by dark- (green) and light- (yellow) colored atoms, respectively.

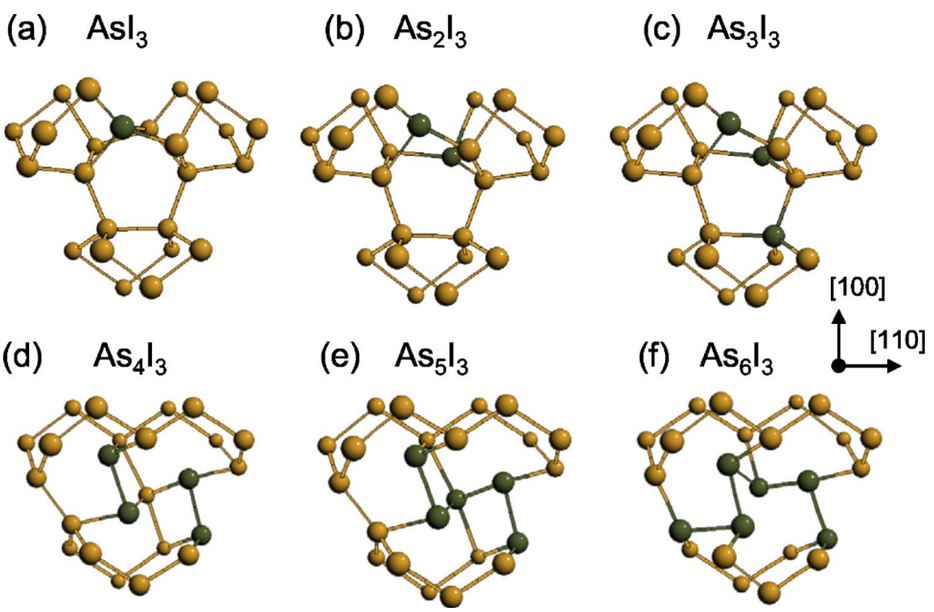


**Figure 3.** (Color online) $As_mI_3$ complex structures. The arsenic and silicon atoms are given by dark- (green) and light- (yellow) colored atoms, respectively.

4. For a given position of the Fermi level, taking into account possible charging of these complexes alters some of their formation energies. For example, the AsI pair is predicted to be more favorable in the negative charge state in heavily As-doped extrinsic regions.[13] Nonetheless, the large binding energies of neutral states suggest stable As-interstitial complex formation. Thus, the potential energy map based on the neutral-state complexes is sufficient in demonstrating the formation of stable As-interstitial complexes. This may in turn provide a physical picture of interstitial-mediated arsenic agglomeration, although further kinetic modeling is required for determination of viable reaction pathways.

The potential energy variation demonstrates the existence of stable As-interstitial clusters as well as As-vacancy clusters. Our earlier first-principles calculations predict the diffusion of an AsI pair to occur with a moderate barrier 0.1–0.4 eV,[13] while the AsV diffusion barrier was predicted to be 1.4 eV[3]. Based on the predicted values, we could expect that AsI and AsV pairs are fairly mobile at high annealing temperatures ($>1000$ K). This in turn suggests that As clustering can be mediated by both vacancies and interstitials. In the presence of excess interstitials, however, As-vacancy complexes (which may form in vacancy-rich regions at the early stage of postimplantation annealing) are eventually annihilated by vacancy-interstitial recombination, and subsequently As-interstitial clusters form due to the binding of interstitials and AsI pairs.

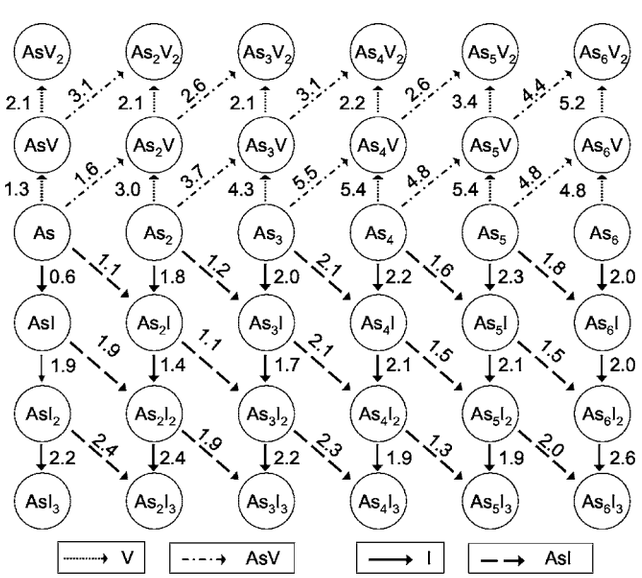


**Figure 4.** A potential energy map of arsenic-defect complexes based on the formation energies presented in Table I. The mobile complexes V, AsV, I, and AsI are represented by the different types of arrows (as shown above), with respective energy gains for the binding of each mobile species noted above each arrow.

Given the fact that As implantation yields excess interstitials, we expect that As-interstitial clusters will be predominant at the stage of As cluster growth during thermal processing. As the density of interstitials decreases during annealing (because of surface annihilation and/or interstitial-vacancy recombination), the As-interstitial complexes will release interstitials, leaving defect-free As complexes.

The substitutional As agglomerates tend to emit lattice Si atoms, with As-vacancy complexes forming upon high-temperature thermal treatment. We determine that $As_3$, $As_4$, and $As_5$ complexes can each emit a lattice Si atom to form As-vacancy complexes at a cost of 3.08, 2.02, and 2.04 eV, respectively. Such interstitial ejection during arsenic deactivation has been established experimentally.[24] In addition, a previous theoretical study suggested interstitial ejection during the formation of As-vacancy complexes.[25] As a whole, our study suggests there is a viable route for interstitial-mediated As deactivation in highly As implanted regions during postimplantation annealing.

In summary, we have identified an interstitial-mediated pathway by which As dopants can agglomerate and form deactivated As-vacancy complexes during junction processing. This pathway includes (*i*) the formation of As-interstitial complexes in the presence of excess interstitials, (*ii*) interstitial emission from these complexes as the interstitial concentration decreases during annealing, and ultimately (*iii*) lattice silicon ejection to form As-vacancy complexes. To illustrate this, we first determine the minimum energy structures and formation energies for As-interstitial complexes ($As_mI_n$, $m \leq 6$ and $n \leq 3$) as well as those for previously identified As-vacancy complexes. We then use these formation energies to form a complete potential energy map of the As-defect complexes that may exist during junction processing. This map shows that the As clustering responsible for As electrical deactivation can occur via both vacancy- and interstitial-mediated pathways. However, we expect

the interstitial-mediated route to dominate, considering that excess interstitials are present at the onset of postimplantation annealing. Our results provide support that interstitials are a determining factor in understanding the kinetic behavior of implanted As dopants during junction formation.

## Acknowledgments

G.S.H. greatly acknowledges the Welch Foundation (F-1535), the International SEMATECH (AMRC-309382), and the NSF (CAREER-CTS-0449373 and ECS-0304026) for their partial financial support. S.A.H. thanks the NSF for support in the form of a graduate research fellowship and the University of Texas for their support in the form of a continuing doctoral fellowship. We would also like to acknowledge the Texas Advanced Computing Center for use of their computing resources.

## References

1. P. M. Rousseau, P. B. Griffin, W. T. Fang, and J. D. Plummer, *J. Appl. Phys.*, **84**, 3593 (1998).
2. K. C. Pandey, A. Erbil, G. S. Cargill III, and R. F. Boehme, *Phys. Rev. Lett.*, **61**, 1282 (1988).
3. M. Ramamoorthy and S. T. Pantelides, *Phys. Rev. Lett.*, **76**, 4753 (1996).
4. D. C. Mueller, E. Alonso, and W. Fichtner, *Phys. Rev. B*, **68**, 045208 (2003).
5. D. W. Lawther, U. Myler, P. J. Simpson, P. M. Rousseau, P. B. Griffin, and J. D. Plummer, *Appl. Phys. Lett.*, **67**, 3575 (1995).
6. V. Ranki, J. Nissila, and K. Saarinen, *Phys. Rev. Lett.*, **88**, 105506 (2002).
7. V. Ranki, K. Saarinen, J. Fage-Pederson, J. Lundsgaard Hansen, and A. Nylandsted Larsen, *Phys. Rev. B*, **67**, 041201R (2003).
8. R. Pinacho, M. Jaraiz, P. Castrillo, I. Martin-Bragado, J. E. Rubio, and J. Barbolla, *Appl. Phys. Lett.*, **86**, 252103 (2005).
9. M. D. Giles, *J. Electrochem. Soc.*, **138**, 1160 (1991).
10. A. Ural, P. B. Griffin, and J. D. Plummer, *J. Appl. Phys.*, **85**, 6440 (1999).
11. R. Kim, T. Hirose, T. Shano, H. Tsuji, and K. Taniguchi, *Jpn. J. Appl. Phys., Part 1*, **41**, 227 (2002).
12. S. Solmi, M. Ferri, M. Bersani, D. Giubertoni, and V. Soncini, *J. Appl. Phys.*, **94**, 4950 (2003).
13. S. A. Harrison, T. F. Edgar, and G. S. Hwang, *Appl. Phys. Lett.*, **87**, 231905 (2004).
14. S. A. Harrison, T. F. Edgar, and G. S. Hwang, *Appl. Phys. Lett.*, **85**, 4935 (2004).
15. K. S. Jones, D. Downey, H. Miller, J. Chow, M. Puga-Lambers, K. Moller, M. Wright, E. Heitman, J. Glassberg, M. Law, L. Robertson, and R. Brindos, in *Proceedings of the International Conference on Ion Implantation Technology*, IEEE, p. 841, Piscataway, NJ (1998).
16. R. Brindos, P. Keys, K. S. Jones, and M. E. Law, *Appl. Phys. Lett.*, **75**, 229 (1999).
17. J. P. Perdew and Y. Wang, *Phys. Rev. B*, **45**, 13244 (1992).
18. G. Kresse and J. Hafner, *Phys. Rev. B*, **47**, RC558 (1993); G. Kresse and J. Furthmuller, *Phys. Rev. B*, **54**, 11169 (1996).
19. D. Vanderbilt, *Phys. Rev. B*, **41**, 7892 (1990).
20. H. J. Monkhorst and J. D. Pack, *Phys. Rev. B*, **13**, 5188 (1976).
21. D. A. Richie, J. Kim, S. A. Barr, K. R. A. Hazzard, R. Hennig, and J. W. Wilkins, *Phys. Rev. Lett.*, **92**, 045501 (2004).
22. G. M. Lopez and V. Fiorentini, *Phys. Rev. B*, **69**, 155206 (2004).
23. S. A. Harrison, T. F. Edgar, and G. S. Hwang, *Phys. Rev. B*, **72**, 195414 (2005).
24. P. M. Rousseau, P. B. Griffin, and J. D. Plummer, *J. Appl. Phys.*, **67**, 3575 (1998).
25. J. Xie and S. P. Chen, *J. Appl. Phys.*, **87**, 4160 (2000).